Electronic Supplementary Material (ESI) for Journal of Materials Chemistry B.

Self-healing and anti-freezing graphene-hydrogel-graphene sandwich strain sensor with ultrahigh sensitivity

Lu Wu[1], Mingshuai Fan[1], Meijie Qu[1], Shuaitao Yang[2], Jia Nie[1], Ping Tang[1], Lujun Pan[2], Hai Wang[1*], Yuezhen Bin[1*]

[1] Department of Polymer Science and Engineering, School of Chemical Engineering, Dalian University of Technology, Dalian, 116024, P. R. China. E-mail: binyz@dlut.edu.cn, haiwang@dlut.edu.cn

[2] School of Physics, Dalian University of Technology, Dalian, 116024, P. R. China.

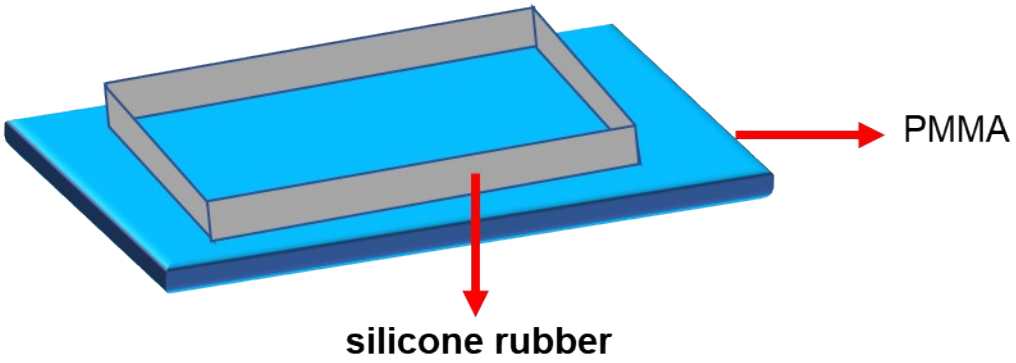

Fig. S1. Schematic diagram of mold for preparing graphene deposited layer

Table S1. Compositions of various composite hydrogel samples

Samples	AA (g)	PVA (g)	Water (g)	Glycerol (g)	Fe^{3+} [b] (mol%)	APS (g)	TEMED (μL)
PVA-4/PAA-1	6.66	2.0	9.5	9.5	0.5	0.05	25
PVA-4/PAA-2	6.66	2.0	9.5	9.5	0.1	0.05	25
PVA-4/PAA-3	6.66	2.0	9.5	9.5	0.15	0.05	25
PVA-4/PAA-4	6.66	2.0	9.5	9.5	0.2	0.05	25

[b] Fe^{3+} (mol%) = [mol (Fe^{3+})/mol (AA)] ×100%

Table S2. Compositions of various composite hydrogel samples

Samples	AA (g)	PVA (g)	Water (g)	Glycerol (g)	Fe^{3+} [b] (mol%)	APS (g)	TEMED (μL)
PVA-1/PAA-1	6.66	0.5	9.5	9.5	0.5	0.05	25
PVA-2/PAA-2	6.66	1.0	9.5	9.5	0.1	0.05	25
PVA-3/PAA-3	6.66	1.5	9.5	9.5	0.15	0.05	25
PVA-4/PAA-4	6.66	2.0	9.5	9.5	0.2	0.05	25

[b] Fe^{3+} (mol%) = [mol (Fe^{3+})/mol (AA)] ×100%

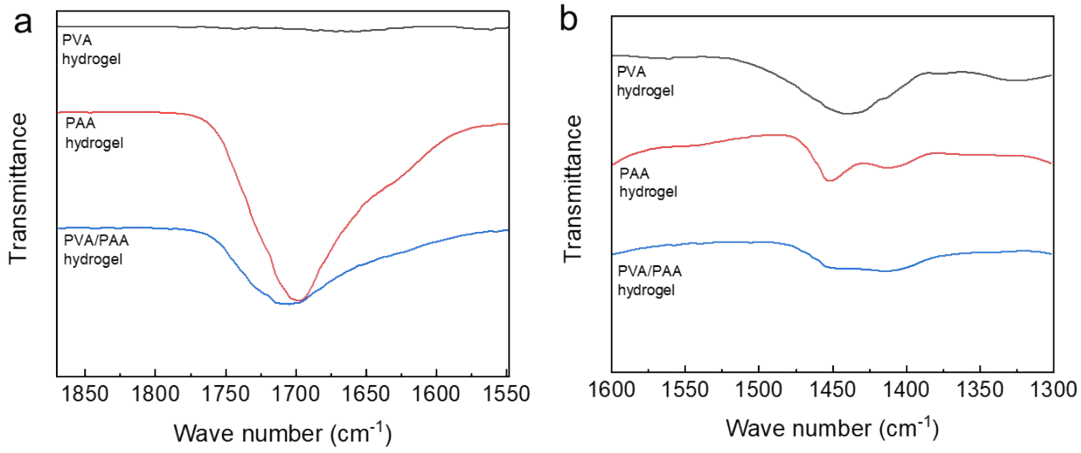

Fig. S2 Partial amplification of FTIR spectra of hydrogel

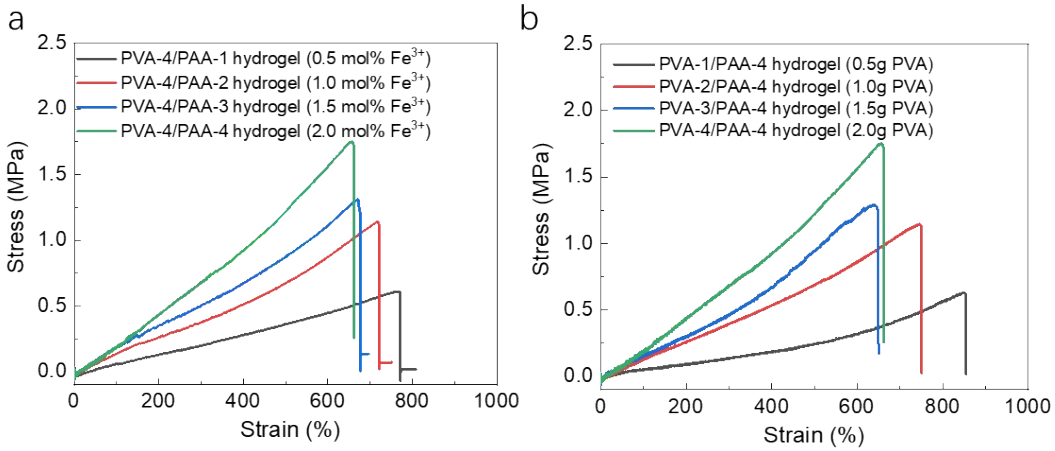

Fig. S3 (a)Effect of Fe^{3+} concentration on mechanical properties of PVA/PAA hydrogel. (b) Effect of PVA content on mechanical properties of PVA/PAA hydrogel

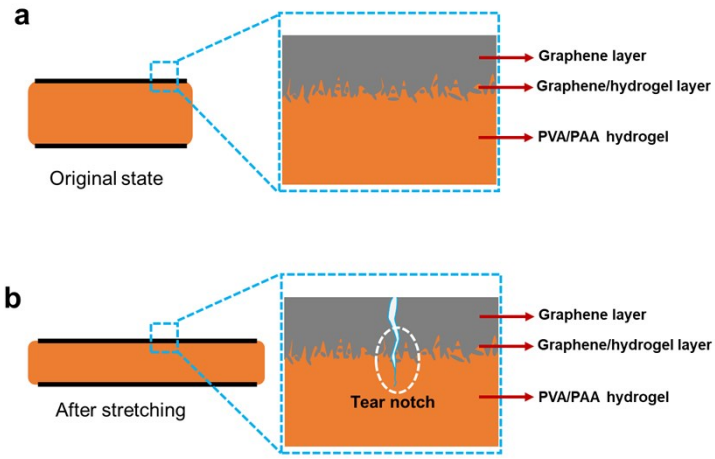

Fig. S4 Changes of surface structure of G-hydrogel-G sandwich sensor during stretching

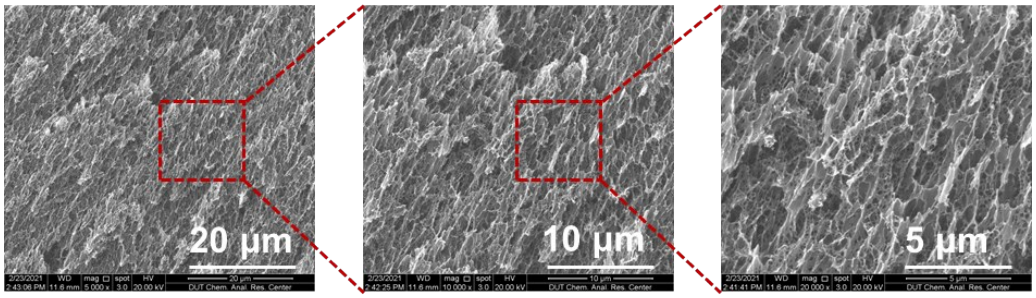

Fig. S5 SEM images of PVA-4/PAA-4 hydrogel

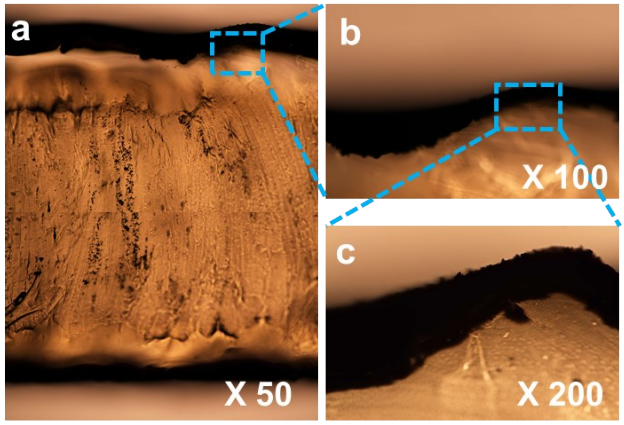

Fig. S6 Optical micrographs[a] of sandwich strain sensor

a: Due to the large magnification of the microscope, the complete cross-sectional structure cannot be observed directly. Therefore, the upper and lower layers of the sensor cross section are independently observed with an optical microscope, then the two photos are combined into a complete cross-sectional optical micrograph.

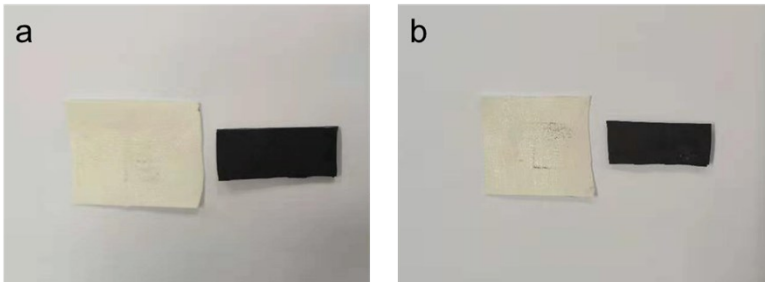

Fig. S7 Adhesion stability of graphene layer. (a) original G-hydrogel-G sandwich sensor, (b) G-hydrogel-G sandwich sensor stored at room temperature for 10 days

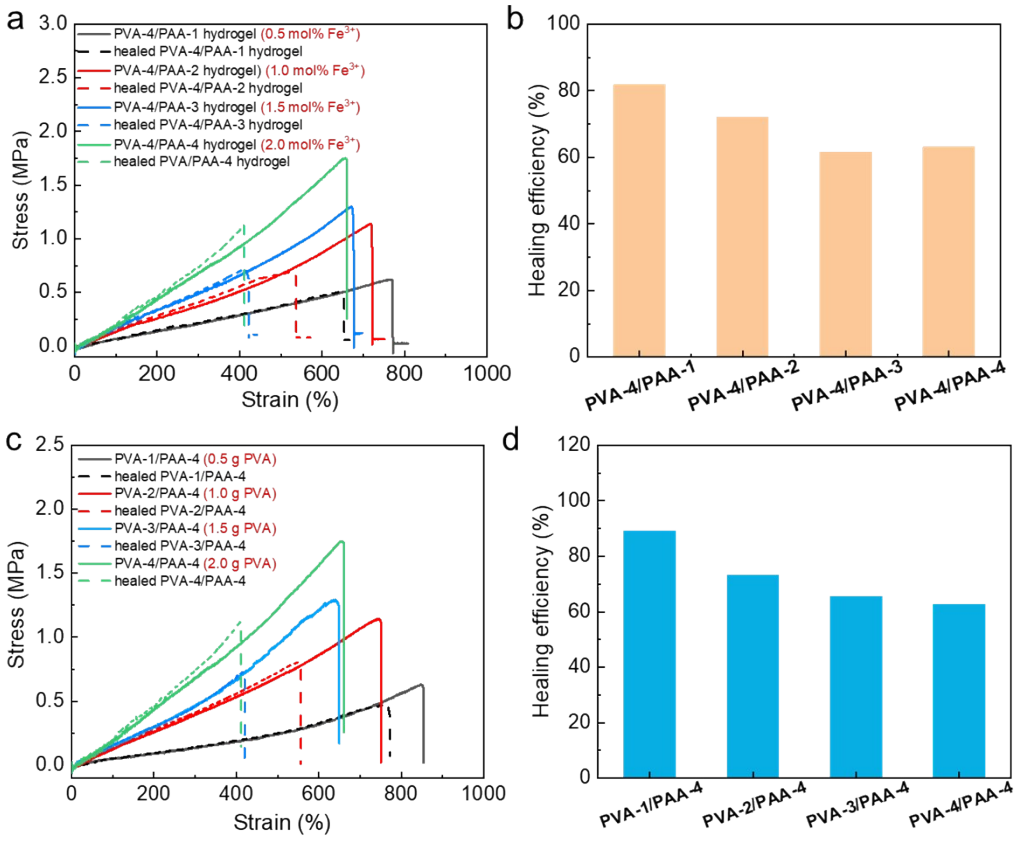

Fig. S8 (a and b) Effect of Fe^{3+} concentration on self-healing properties of PVA/PAA hydrogel. (c and d) Effect of PVA content on self-healing properties of PVA/PAA hydrogel

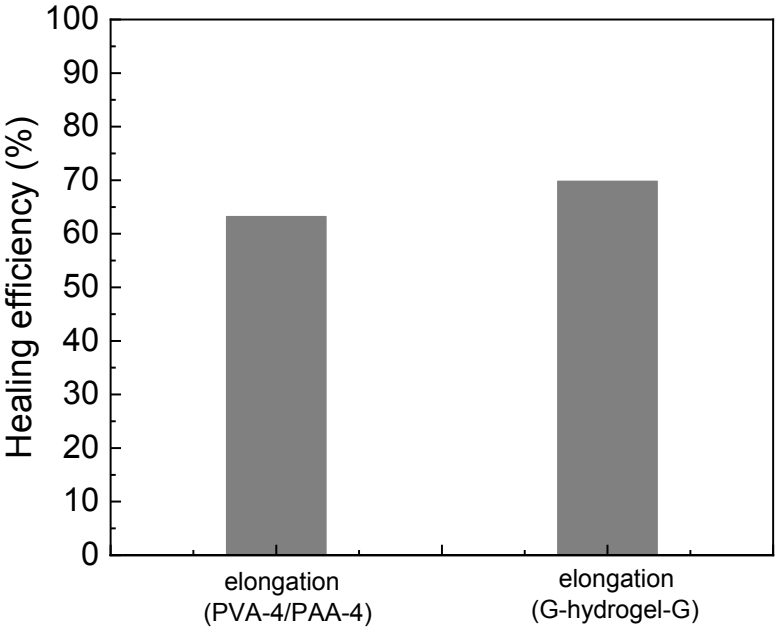

Fig. S9 The self-healing efficiency of PVA-4/PAA-4 hydrogel and G-hydrogel-G sandwich strain sensor

Table S3 Raw material compositions of PVA/PAA-W hydrogel

Sample	PVA (g)	Glycerol (g)	Water (g)	AA (g)	Fe^{3+b} (mol%)	APS (μL) (0.5 g/mL)
PVA/PAA-W	2.0	0	19	6.66	1	50

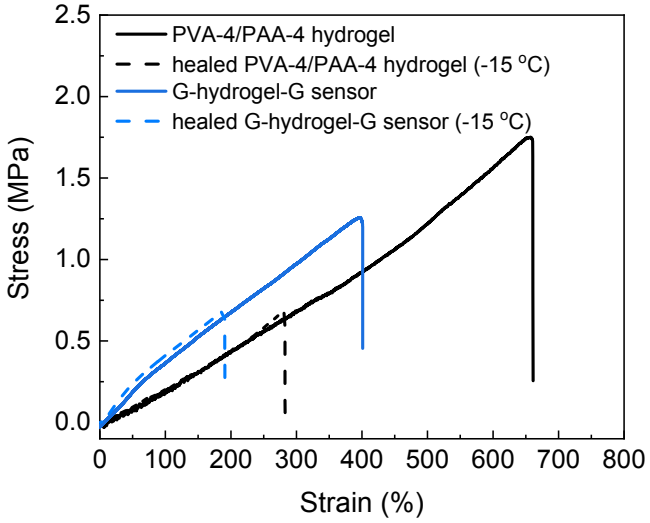

Fig. S10 Self-healing efficiency of PVA-4/PAA-4 hydrogel and G-hydrogel-G sandwich strain sensor at -15 ℃

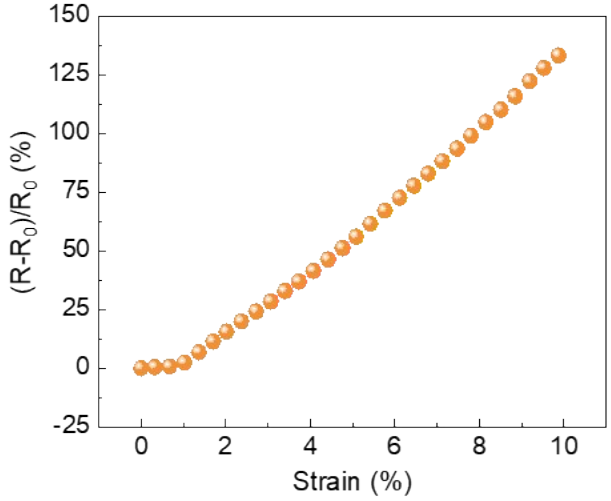

Fig. S11 Relationships between resistance change and strain (<10% deformation)

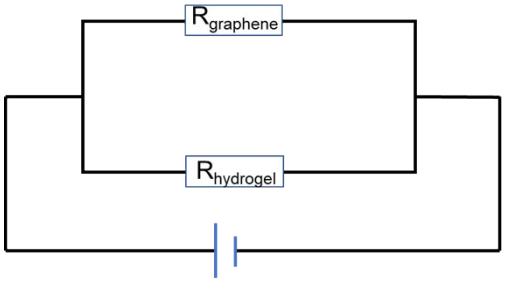

Fig. S12 Working mechanism of the sandwich strain sensor

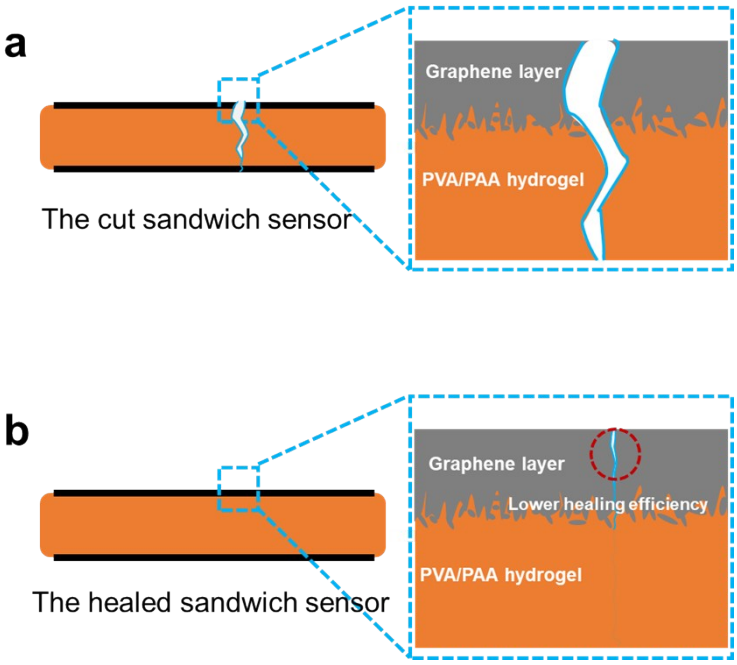

Fig. S13 Healing process of sandwich sensor